

*Rapid Commun. Mass Spectrom.* 2011, 25, 1801–1811  
(wileyonlinelibrary.com) DOI: 10.1002/rcm.5045

# Characterization of carbonyl by-products during Uniblu-A ozonation by liquid chromatography/hybrid quadrupole time-of-flight/mass spectrometry

A. Amorisco, V. Locaputo and G. Mascolo\*

Istituto di Ricerca Sulle Acque, Consiglio Nazionale delle Ricerche, Viale F. De Blasio 5, 70132 Bari, Italy

The structural elucidation of carbonyl-containing by-products arising from Uniblu-OH ozonation has been investigated by liquid chromatography/electrospray ionization tandem mass spectrometry (LC/ESI-MS/MS) employing a quadrupole time-of-flight mass spectrometer. The by-products were derivatized with 2,4-dinitrophenylhydrazine, allowing the formation of  $[M-H]^-$  ions of the derivatives in the electrospray source. Exact mass measurements of both the  $[M-H]^-$  ions and their product ions allowed the elemental formulae and related structures of ten by-products to be determined confidently. The main degradation pathway were decarboxylation followed by further oxidation. It is noteworthy that the experimental procedure employed allowed the identification of both nitrogen- and sulphur-containing carbonyl by-products during Uniblu-OH ozonation. This result is of environmental relevance for monitoring the balance of organic nitrogen and sulphur during the ozonation of organic pollutants. These atoms, in fact, do not undergo complete mineralization. Copyright © 2011 John Wiley & Sons, Ltd.

Textile dyes and other dyestuffs represent a major source of industrial water pollution in many countries due to their persistence, acute toxicity or mutagenic effects to exposed aquatic organisms. A major issue of discussion and regulation in the developed countries is the removal of color from textile wastewater, also including the requirement to recycle the rinsing water from dye baths.

Conventional textile wastewater treatment plants that rely on biological oxidation (biodegradation)<sup>[1]</sup> and/or simple physicochemical (adsorption)<sup>[2]</sup> strategies are ineffective in achieving complete decolorization and the removal of dye residues because most dyestuffs are both resistant to biological degradation and highly water soluble. It follows that the employment of more powerful chemical methods, namely those known as advanced oxidation processes (AOPs), is necessary to reach the target legal limit for effluent discharge. AOPs are chemical methods based on the generation of hydroxyl radicals ( $\bullet OH$ ) able to oxidize contaminants in a non-selective manner.<sup>[3–8]</sup>

It has been reported that ozonation is one of the most effective technologies for the remediation of textile wastewater containing bio-recalcitrant dyes and other persistent organic compounds.<sup>[9,10]</sup> Several studies have been carried out that demonstrate the efficiency of ozone treatment for removal of dyes and some of them were also aimed at identifying the resulting by-products.<sup>[11–15]</sup> Due to its high oxidation potential, ozone can effectively break down the conjugated double

bonds of the chromophores of dyestuffs as well as other functional groups such as their complex aromatic rings.<sup>[16–18]</sup> This ultimately leads to the formation of smaller molecules with fewer conjugated double bonds, thereby decreasing the color of effluent. However, although the removal of dyes by ozonation is often successfully achieved, their complete oxidation (i.e., the total mineralization of organic carbon to carbon dioxide) is seldom obtained. Therefore, ozonation by-products should usually be expected in ozonation effluents.

Reactive dyestuffs based on the anthraquinone structure have long been used in cellulose fiber dyeing. They are more resistant to biodegradation due to their fused aromatic structures than azo-based dyes.<sup>[19]</sup> The anthraquinone-based dyes represent an environmental problem as it is not possible to recover them from spent baths because the reaction carried out to link them to fibers leads to the formation, through a side reaction, of the hydrolyzed dyes. As the fixation rate between the reactive dye and the fiber is usually below 90% it follows that the resulting spent waters cannot be further used and should be disposed of properly. However, little information about the ozonation products of anthraquinone reactive dyes is available.<sup>[20–25]</sup> In general, as degradation by-products are more polar than the parent compounds their identification is often carried out by liquid chromatography/electrospray ionization mass spectrometry (LC/ESI-MS), often employing accurate mass measurement.<sup>[26,27]</sup> It is known that such by-products are transient compounds as they are further degraded, leading to the formation of low molecular weight carbonyl compounds which, in turn, are finally degraded to low molecular weight organic acids. However, the identification of low molecular weight aldehydes and ketones only on the basis of comparison with authentic standards fails to account for the total organic carbon present in the ozonated aqueous solution.<sup>[28]</sup> It follows that unknown low molecular

\* Correspondence to: G. Mascolo, Istituto di Ricerca Sulle Acque, Consiglio Nazionale delle Ricerche, Viale F. De Blasio 5, 70132 Bari, Italy.  
E-mail: giuseppe.mascolo@ba.irsra.cnr.it

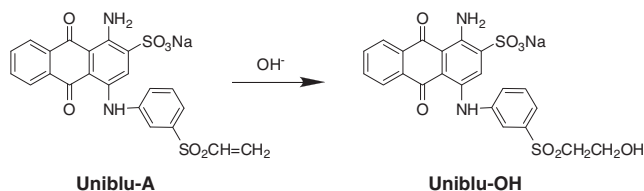
weight carbonyl compounds are present in these ozonation products. The unequivocal identification of these compounds should be possible by LC/ESI-MS combined with accurate mass measurement, both in single and tandem MS, using quadrupole time-of-flight mass spectrometry (QqTOFMS). In order to achieve such a goal it is mandatory to employ a preliminary derivatization step, for example by using 2,4-dinitrophenylhydrazine (DNPH) to form hydrazone derivatives, as reported in many applications such as the study of automobile and cigarette exhaust samples,<sup>[29]</sup> beer,<sup>[30]</sup> ozonated drinking waters and outdoor swimming pools,<sup>[31]</sup> and biological matrices including urine<sup>[32–34]</sup> and exhaled breath.<sup>[35]</sup>

The aim of the present investigation was the unequivocal characterization of aldehydes and ketones, formed during the ozonation of hydrolyzed Uniblu-A (Uniblu-OH) at longer contact times, by accurate mass MS and MS/MS determination using LC/ESI-QqTOFMS after the derivatization of the compounds with DNPH.

## EXPERIMENTAL

### Chemicals

Uniblu-A (95% purity; Aldrich, Milwaukee, WI, USA) was used without further purification. Uniblu-OH was obtained by hydrolyzing an aqueous solution of Uniblu-A (500 mg/L) at pH 12 and 50°C for 1 h (hydrolysis yield >90%) as reported below.



Solvents used for high-pressure liquid chromatography (HPLC) were HPLC-MS grade and purchased from Sigma-Aldrich (St. Louis, MO, USA). Water used for liquid chromatography as well as for preparing all standard aqueous solutions (18.2 MΩcm, organic carbon content  $\leq 4 \mu\text{g/L}$ ) was obtained from a Milli-Q Gradient A-10 system (Millipore, Billerica, MA, USA). 2,4-Dinitrophenylhydrazine (DNPH; purity  $\geq 99\%$ ) was purchased from Aldrich. All other reagents were analytical grade and purchased from VWR (West Chester, PA, USA) or Carlo Erba (Milan, Italy).

### Ozonation experiments

A volume of 500 mL of a Uniblu-OH aqueous solution (the pH was adjusted to 7 with HCl) was placed into a Normag reactor (Normag, Limenau, Germany). Ozone was produced by a Fisher 502 ozonator (Meckenheim, Germany) fed with oxygen. The oxygen/ozone mixture (1 L/min, 16 mg/L) was split to allow just 0.1 L/min to be bubbled into the Normag reactor. The ozone output was monitored before each experiment by determining (by titration with sodium thiosulfate) the amount of free iodine liberated from a potassium iodide solution. Samples (10 mL) were withdrawn from the reaction mixtures at scheduled times and the residual ozone was stripped by

purging with air. They were then subjected to derivatization with DNPH according to a published procedure<sup>[36,37]</sup> in order to determine the aldehydes and ketones by LC/MS. Briefly, 50 mL of an aqueous sample was buffered to pH 3 with citrate buffer and 3 mL of a DNPH aqueous solution (3 g/L) was added. The compounds were derivatized at 40°C for 1 h. The aqueous phase was then analyzed by LC/MS.

### LC/ESI-QqTOFMS and LC/ESI-QqTOFMS/MS analysis

A QSTAR QqTOFMS/MS system (AB Sciex, Foster City, CA, USA) equipped with a TurboIonSpray source operated in negative ion mode was used throughout this work. High-purity nitrogen gas was used as the curtain and collision gas, while high-purity air was used as the nebulizer and auxiliary heated gas. The TurboIonSpray interface conditions were as follows: nebulizer voltage, -4200 V; declustering potential, -20 V; focusing potential, -100 V; nebulizer gas flow rate, 1 L/min; curtain gas flow rate, 1 L/min; auxiliary gas (air) flow delivered by a turbo heated probe, at 8 L/min at 350°C. Samples injected by a series 200 autosampler (Perkin-Elmer, Waltham, MA, USA), equipped with a 9010 Rheodyne valve and a 200  $\mu\text{L}$  loop, were eluted at 0.6 mL/min through an Alltima 5 mm C18 reversed-phase column (250  $\times$  3.2 mm; Alltech, Deerfield, IL, USA) and C18 precolumn (4  $\times$  2.0 mm; Phenomenex, Macclesfield, UK) with the following gradient, delivered by three series 200 micro-LC pumps (Perkin-Elmer): from 85:5:10 (water/CH<sub>3</sub>CN/CH<sub>3</sub>COOH 1% in CH<sub>3</sub>CN) to 10:80:10 in 20 min, which was then held for 5 min. The flow from the LC pumps was split 1:1, by means of a zero dead volume T-piece, to allow one-half to enter the TurboIonSpray interface. A few analyses were also performed using two C18 Chromolith columns (Merck, Darmstadt, Germany) connected in series at 1 mL/min using the same above-reported gradient. In this case the flow from the LC pumps was split 1:2.

Accurate mass measurements (four decimal places) were carried out at a mass resolution higher than 5000 (full width at half maximum) by obtaining averaged spectra from chromatographic peaks and by then recalibrating them using the [M-H]<sup>-</sup> ions of polyacrylic acid injected post-column (C<sub>9</sub>H<sub>13</sub>O<sub>4</sub><sup>-</sup>, C<sub>12</sub>H<sub>17</sub>O<sub>6</sub><sup>-</sup> and C<sub>15</sub>H<sub>21</sub>O<sub>8</sub><sup>-</sup> at *m/z* 185.08193, 257.10306 and 329.12419, respectively). Accurate mass product ion measurements (four decimal places) were carried out by fragmenting the target (precursor) [M-H]<sup>-</sup> ions of the selected DNPH derivative at an optimized collision energy (CE) and at a collision gas pressure of 4 mTorr. Each averaged spectrum was recalibrated using, as a lock mass, the precursor ion mass obtained in single MS mode or the product ion at *m/z* 182.0207 ([M-H]<sup>-</sup> ion of 2,4-dinitroaniline) which is the typical product ion deriving from the derivatization agent, or both these masses. The CE was optimized for each deprotonated DNPH derivative by-product in order to obtain, where possible, spectra showing acceptable signal-to-noise (S/N) ratios in the MS/MS spectra, with both the [M-H]<sup>-</sup> ion and the highest number of product ions being of high enough abundance for accurate mass determination. All MS data handling was performed using Analyst QS software (AB Sciex).

## RESULTS AND DISCUSSION

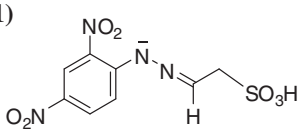
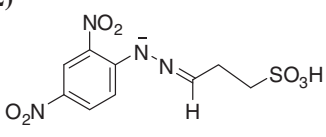
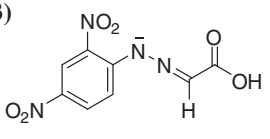
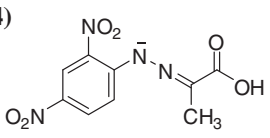
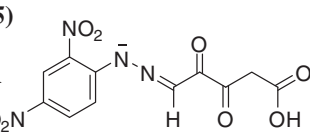
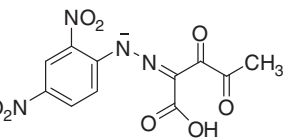
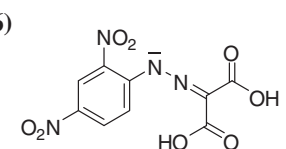
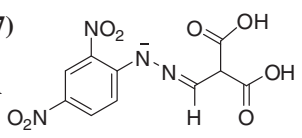
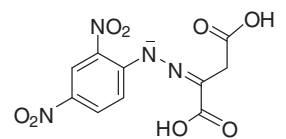
The reaction of Uniblu-OH with ozone led to the quick disappearance of the parent compound. At the same time, a number of by-products were formed as a result of oxidation reactions of the amino group, of the aromatic rings of the anthraquinone nucleus and/or of the benzenesulfoxide groups. Competitive reactions such as the hydrolysis of the 2-hydroxyethylsulfonyl and benzenesulfoxide groups can be invoked to explain the formation of the already detected by-products.<sup>[28]</sup> It is worth noting that such by-products were mainly identified at short ozonation times and disappeared completely at reaction times longer than 15 min. At such reaction times no by-product was detectable by HPLC-UV-MS but several low molecular weight DNPH-aldehydes were detected on the basis of authentic standards (formaldehyde, acetaldehyde, glyoxal, propanal, 2-propenal, propanone, butanal, butanone, 2-butenal). However, these compounds failed to account for the whole organic matter left in the reaction mixture suggesting the presence of unidentified aldehydes and ketones. Indeed, some of them are also likely to be sulfur-containing aldehydes, on the basis of the finding that the amount of mineralized sulfur (i.e. inorganic sulfate) fails to account for the total organic sulphur of Uniblu-OH present at the beginning of the reaction. Employing the derivatization procedure with DNPH ten unknown by-products were identified on the basis of accurate mass measurements of both the  $[M-H]^-$  ions and their main product ions, as listed in Table 1. As expected, all the derivatized by-products gave a characteristic product ion at  $m/z$  182, corresponding to the  $[M-H]^-$  ion of 2,4-dinitroaniline, as a consequence of the derivatization procedure with DNPH. Therefore, this ion was usefully employed as a lock mass, as mentioned in the Experimental section. It is worth noting that the mass measured  $[M-H]^-$  ions reported in Table 1 often have associated errors of a few ppm due to the employed QqTOFMS instrumentation. However, this did not prevent the elemental composition being unequivocally assigned. In fact, if no atom constraints were set several possible elemental compositions are possible for each by-product within 6 ppm error for mass accuracy. Instead, by considering the additional information that each by-product had previously been derivatized by DNPH it was possible to apply proper atom and DBE constraints ( $C \geq 6$ ,  $H \geq 3$ ,  $O \geq 4$ ,  $N \geq 4$ ,  $S \geq 0$ ,  $DBE \geq 7.5$ ) leading to obtaining a single or a couple of possible elemental compositions for each compound (Supplementary Fig. S1, Supporting Information). Further, when two elemental compositions were obtained, we found that one was not chemically consistent due to the low number of hydrogen atoms. Therefore, for all the derivatized by-products a single elemental composition was confidently obtained although the mass accuracy error was about 6 ppm.

By-products 1 and 2 showed  $[M-H]^-$  ions at  $m/z$  303.0038 and 317.0217, consistent with elemental compositions  $C_8H_7N_4O_7S^-$  and  $C_9H_9N_4O_7S^-$  (error -1.0 and 6.2 ppm, respectively) indicating a methylene group difference between the two compounds. Their MS/MS spectra (Fig. 1(a) and Supplementary Fig. S1, Supporting Information) show product ion at  $m/z$  80.9648 and 80.9681 attributed to  $HSO_3^-$  (error -4.8 and 35.8 ppm for by-product 1 and 2, respectively), suggesting that these compounds are sulfur-containing by-products. The high error in the measurement of the  $HSO_3^-$  product ion from

by-product 2 is probably due to its low intensity. Close examination of the product ion spectrum of the deprotonated by-product 1 (Fig. 1(a)) reveals other minor product ions at  $m/z$  223.0512 and 257.0130, corresponding to  $C_8H_7N_4O_4^-$  and  $C_8H_7N_3O_5S^-$ , respectively. The ion at  $m/z$  223 is formed through the loss of  $SO_3$  from the precursor ion. This ion then gives rise to the  $[M-H]^-$  ion of 2,4-dinitroaniline ( $m/z$  182) through loss of acetonitrile. The radical anion at  $m/z$  257 represents the competitive loss of nitrous acid from the deprotonated molecule followed by a proton shift. All the information obtained from the product ion spectrum was rationalized in the fragmentation pathway depicted in Fig. 2, leading to the conclusion that by-product 1 is a 2-oxoethanesulfonic acid, DNPH derivatized in position 2. It is formed by loss of 2-hydroxyethanesulfonic acid from Uniblu-OH and then oxidation of the ethoxy group.

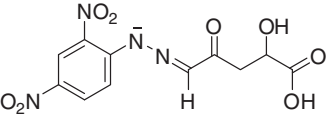
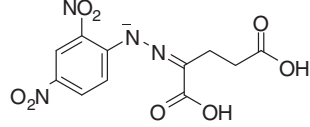
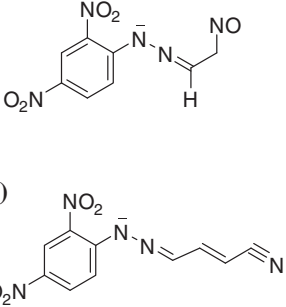
The product ion mass spectrum of deprotonated by-product 2 (Supplementary Fig. S1, Supporting Information) revealed only an additional product ion at  $m/z$  96.9600, assigned to  $HSO_4^-$  (error -1.1 ppm). On the basis of such few observed product ions, the structure of by-product 2 is proposed as 3-oxopropane-1-sulfonic acid, DNPH derivatized in position 3 (Supplementary Fig. S2, Supporting Information). This compound is formed by cleavage of the 2-hydroxyethylsulfonyl group of Uniblu-OH and oxidation of the hydroxyl moiety. From Table 1 it can be seen that many of the by-products (3–8) formed product ions through neutral loss of 44 Da, generally indicating the presence of a carboxylic acid group. The  $[M-H]^-$  ions of by-products 3 and 4 were at  $m/z$  253.0208 and 267.0364 with elemental compositions of  $C_8H_5N_4O_6^-$  (error -2.6 ppm) and  $C_9H_7N_4O_6^-$  (error -2.6 ppm), respectively. Their structures were assigned as the DNPH derivatives of 2-oxoacetic acid and 2-oxopropanoic acid, i.e. an aldehyde and a saturated ketone, respectively. The product ion spectra of these by-products were mainly dominated by the  $m/z$  182 ion (Supplementary Figs. S3 and S5, Supporting Information) and had similar fragmentation pathways. Specifically, the deprotonated molecules yield product ions at  $m/z$  209.0363 and 223.0504, neutral loss of  $CO_2$  and then the base peak (the  $[M-H]^-$  ion of 2,4-dinitroaniline at  $m/z$  182) through  $CH_3CN$  loss and hydrogen shift (Fig. 3 and Supplementary Fig. S4, Supporting Information). This product ion, in turn, gives rise to an ion at  $m/z$  152, an odd-electron ion consistent with an elemental composition of  $C_6H_4N_2O_3^-$ , formed by loss of a NO radical (30 Da). It has been reported that product ions originating from the DNPH moiety might be affected by the structure of the respective carbonyl compound, making it possible to distinguish between aliphatic aldehydes (product ion at  $m/z$  163 and less abundant ion at  $m/z$  179), aldehydes and ketones (intense  $m/z$  152 product ion) and dicarbonyl compounds (intense  $m/z$  182 product ion).<sup>[38,39]</sup> The product ion spectra of the DNPH derivatives of by-products 3 and 4 (Supplementary Figs. S3 and S5, Supporting Information) revealed a base ion peak at  $m/z$  182 and product ions at  $m/z$  152 and 163 of very low intensity. It follows that the above reported features cannot be applied to compounds having multiple functional groups. Specifically, when the carboxylic group is present together with an aldehyde or a ketone, a very intense  $m/z$  182 product ion (base peak) is observed. This means that in such a situation the dicarbonyl character of the compound prevails in the product ion spectrum over the other characteristics. The product ion at  $m/z$  163.0279 of by-product

**Table 1.** Accurate mass measurements and elemental compositions of degradation products of Uniblu-OH derivatized with DNPH and their product ions using LC/QqTOF-MS and LC/QqTOF-MS-MS analysis

Structures of by-products derivatized by DNPH	Measured mass [M-H] <sup>-</sup>	CE (eV)	Major ions	Elemental composition	Calculated mass	Error (ppm)
(1) 	303.0038	20	<b>303.0038</b>	C <sub>8</sub> H <sub>7</sub> N <sub>4</sub> O <sub>7</sub> S <sup>-</sup>	303.0041	-1.0
			257.0130	C <sub>8</sub> H <sub>7</sub> N <sub>3</sub> O <sub>5</sub> S <sup>-</sup>	257.0112	7.0
			223.0512	C <sub>8</sub> H <sub>7</sub> N <sub>4</sub> O <sub>4</sub> <sup>-</sup>	223.0473	17.5
			182.0207	C <sub>6</sub> H <sub>4</sub> N <sub>3</sub> O <sub>4</sub> <sup>-</sup>	182.0207	LM
			80.9648	HSO <sub>3</sub> <sup>-</sup>	80.9652	-4.8
(2) 	317.0217	15	<b>317.0217</b>	C <sub>9</sub> H <sub>9</sub> N <sub>4</sub> O <sub>7</sub> S <sup>-</sup>	317.0197	6.2
			182.0207	C <sub>6</sub> H <sub>4</sub> N <sub>3</sub> O <sub>4</sub> <sup>-</sup>	182.0207	LM
			96.9600	HSO <sub>4</sub> <sup>-</sup>	96.9601	-1.1
			80.9681	HSO <sub>3</sub> <sup>-</sup>	80.9652	35.8
(3) 	253.0208	15	<b>253.0208</b>	C <sub>8</sub> H <sub>5</sub> N <sub>4</sub> O <sub>6</sub> <sup>-</sup>	253.0215	-2.6
			209.0363	C <sub>7</sub> H <sub>5</sub> N <sub>4</sub> O <sub>4</sub> <sup>-</sup>	209.0316	22.3
			182.0145	C <sub>6</sub> H <sub>4</sub> N <sub>3</sub> O <sub>4</sub> <sup>-</sup>	182.0207	-34.2
			163.0279	C <sub>6</sub> H <sub>3</sub> N <sub>4</sub> O <sub>2</sub> <sup>-</sup>	163.0261	10.7
			152.0240	C <sub>6</sub> H <sub>4</sub> N <sub>2</sub> O <sub>3</sub> <sup>-</sup>	152.0227	8.3
(4) 	267.0364	20	<b>267.0364</b>	C <sub>9</sub> H <sub>7</sub> N <sub>4</sub> O <sub>6</sub> <sup>-</sup>	267.0371	-2.6
			223.0504	C <sub>8</sub> H <sub>7</sub> N <sub>4</sub> O <sub>4</sub> <sup>-</sup>	223.0473	13.9
			197.0328	C <sub>6</sub> H <sub>5</sub> N <sub>4</sub> O <sub>4</sub> <sup>-</sup>	197.0316	5.9
			182.0209	C <sub>6</sub> H <sub>4</sub> N <sub>3</sub> O <sub>4</sub> <sup>-</sup>	182.0207	0.9
			179.0232	C <sub>6</sub> H <sub>3</sub> N <sub>4</sub> O <sub>3</sub> <sup>-</sup>	179.0211	11.9
			167.0335	C <sub>6</sub> H <sub>5</sub> N <sub>3</sub> O <sub>3</sub> <sup>-</sup>	167.0336	-0.8
			163.0288	C <sub>6</sub> H <sub>3</sub> N <sub>4</sub> O <sub>2</sub> <sup>-</sup>	163.0261	16.3
			152.0248	C <sub>6</sub> H <sub>4</sub> N <sub>2</sub> O <sub>3</sub> <sup>-</sup>	152.0227	13.5
(5) 	323.0288	15	<b>323.0288</b>	C <sub>11</sub> H <sub>7</sub> N <sub>4</sub> O <sub>8</sub> <sup>-</sup>	323.0269	5.8
			279.0360	C <sub>10</sub> H <sub>7</sub> N <sub>4</sub> O <sub>6</sub> <sup>-</sup>	279.0371	-3.9
			182.0207	C <sub>6</sub> H <sub>4</sub> N <sub>3</sub> O <sub>4</sub> <sup>-</sup>	182.0207	LM
			96.0064	C <sub>4</sub> H <sub>2</sub> NO <sub>2</sub> <sup>-</sup>	96.0091	-28.1
(5) 						
(6) 	297.0101	20	<b>297.0101</b>	C <sub>9</sub> H <sub>5</sub> N <sub>4</sub> O <sub>8</sub> <sup>-</sup>	297.0113	-4.0
			253.0212	C <sub>8</sub> H <sub>5</sub> N <sub>4</sub> O <sub>6</sub> <sup>-</sup>	253.0215	-1.2
			209.0306	C <sub>7</sub> H <sub>5</sub> N <sub>4</sub> O <sub>4</sub> <sup>-</sup>	209.0316	-4.9
			182.0207	C <sub>6</sub> H <sub>4</sub> N <sub>3</sub> O <sub>4</sub> <sup>-</sup>	182.0207	LM
(7) 	311.0286	15	<b>311.0286</b>	C <sub>10</sub> H <sub>7</sub> N <sub>4</sub> O <sub>8</sub> <sup>-</sup>	311.0269	5.3
			267.0387	C <sub>9</sub> H <sub>7</sub> N <sub>4</sub> O <sub>6</sub> <sup>-</sup>	267.0371	5.9
			223.0476	C <sub>8</sub> H <sub>7</sub> N <sub>4</sub> O <sub>4</sub> <sup>-</sup>	223.0473	1.4
			182.0207	C <sub>6</sub> H <sub>4</sub> N <sub>3</sub> O <sub>4</sub> <sup>-</sup>	182.0207	LM
(7) 						

(Continues)

Table 1. (Continued)

Structures of by-products derivatized by DNPH	Measured mass [M-H] <sup>-</sup>	CE (eV)	Major ions	Elemental composition	Calculated mass	Error (ppm)
<b>(8)</b>  <b>A</b>	325.0442	15	<b>325.0442</b>	C <sub>11</sub> H <sub>9</sub> N <sub>4</sub> O <sub>8</sub> <sup>-</sup>	325.0426	5.0
			281.0536	C <sub>10</sub> H <sub>9</sub> N <sub>4</sub> O <sub>6</sub> <sup>-</sup>	281.0528	3.0
			253.0184	C <sub>8</sub> H <sub>5</sub> N <sub>4</sub> O <sub>6</sub> <sup>-</sup>	253.0215	-12.2
			182.0207	C <sub>6</sub> H <sub>4</sub> N <sub>3</sub> O <sub>4</sub> <sup>-</sup>	182.0207	LM
			179.0219	C <sub>6</sub> H <sub>3</sub> N <sub>4</sub> O <sub>3</sub> <sup>-</sup>	179.0211	4.6
			163.0219	C <sub>6</sub> H <sub>3</sub> N <sub>4</sub> O <sub>2</sub> <sup>-</sup>	163.0261	-26.1
			153.0301	C <sub>6</sub> H <sub>5</sub> N <sub>2</sub> O <sub>3</sub> <sup>-</sup>	153.0306	- 3.0
<b>(9)</b>  <b>B</b>	252.0366	15	<b>252.0366</b>	C <sub>8</sub> H <sub>6</sub> N <sub>5</sub> O <sub>5</sub> <sup>-</sup>	252.0374	-3.3
			209.0318	C <sub>7</sub> H <sub>5</sub> N <sub>4</sub> O <sub>4</sub> <sup>-</sup>	209.0316	0.8
<b>(10)</b>  <b>C</b>	260.0425	10	<b>260.0425</b>	C <sub>10</sub> H <sub>6</sub> N <sub>5</sub> O <sub>4</sub> <sup>-</sup>	260.0425	-0.1
			223.0471	C <sub>8</sub> H <sub>7</sub> N <sub>4</sub> O <sub>4</sub> <sup>-</sup>	223.0473	-0.9
			182.0198	C <sub>6</sub> H <sub>4</sub> N <sub>5</sub> O <sub>4</sub> <sup>-</sup>	182.0207	-5.1

LM: lock mass used to recalibrate the averaged spectrum.

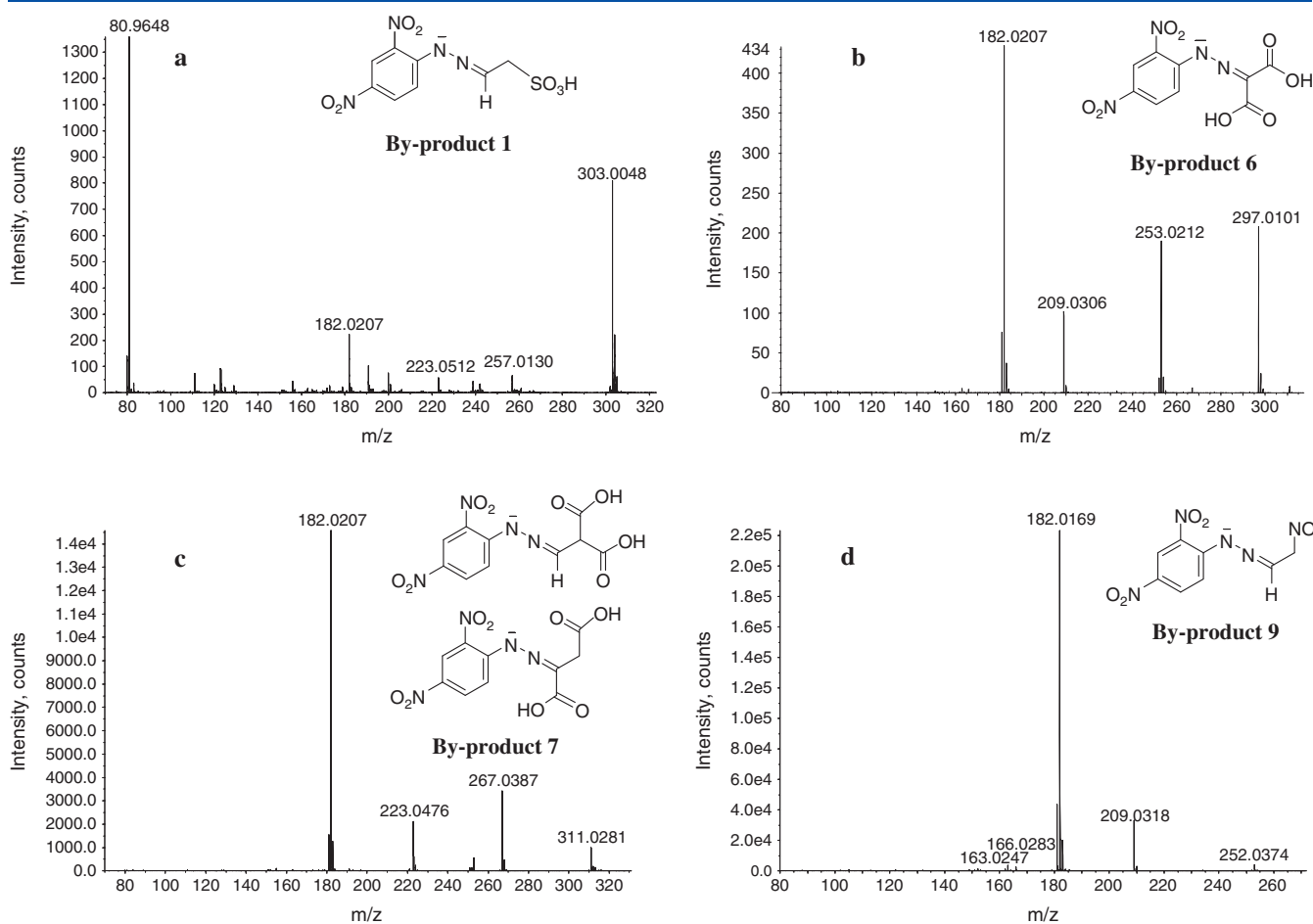
3, typical for aliphatic DNPH-aldehydes, is formed by oxalic acid elimination and a cyclization reaction which stabilizes the formed product ion (Supplementary Fig. S4, Supporting Information). In addition, the formation of an ion at  $m/z$  179.0232 of by-product 4 was assigned to C<sub>6</sub>H<sub>3</sub>N<sub>4</sub>O<sub>3</sub><sup>-</sup> (error 11.9 ppm). Its formation can be rationalized by consecutive loss of ethene (leading to the ion at  $m/z$  197.0328, C<sub>6</sub>H<sub>5</sub>N<sub>4</sub>O<sub>4</sub><sup>-</sup>, error 5.9 ppm) and water from the product ion at  $m/z$  223.0504 (Fig. 3), assigned to acetaldehyde-DNPH, this hypothesis being supported by published data.<sup>[38]</sup> In addition, the proposed structure of by-product 4 was also consistent with its chromatographic behaviour, showing a double peak, as typically found for asymmetric DNPH-ketones.

By-product 5 showed a [M-H]<sup>-</sup> ion at  $m/z$  323.0288 consistent with elemental composition C<sub>11</sub>H<sub>7</sub>N<sub>4</sub>O<sub>8</sub><sup>-</sup> (error 5.8 ppm) for which two possible chemical structures can be proposed (Table 1). The product ion spectrum (Supplementary Fig. S6, Supporting Information) showed, in addition to the intense ion at  $m/z$  182, the formation of a product ion at  $m/z$  279.0360 whose elemental composition is C<sub>10</sub>H<sub>7</sub>N<sub>4</sub>O<sub>6</sub><sup>-</sup> (error -3.9 ppm). This ion can be assigned to deprotonated 2,3-dioxobutanal-DNPH, formed by CO<sub>2</sub> neutral loss, supporting the presence of a mono-carboxylic acid group on this by-product. This ion fragmented further, leading to the ion at  $m/z$  182 and competitively to the ion at  $m/z$  96.0064 assigned to C<sub>4</sub>H<sub>2</sub>NO<sub>2</sub><sup>-</sup> (error -28.1 ppm), as depicted in Supplementary Fig. S7 (see Supporting Information). However, in this case the fragmentation pattern did not allow us to distinguish

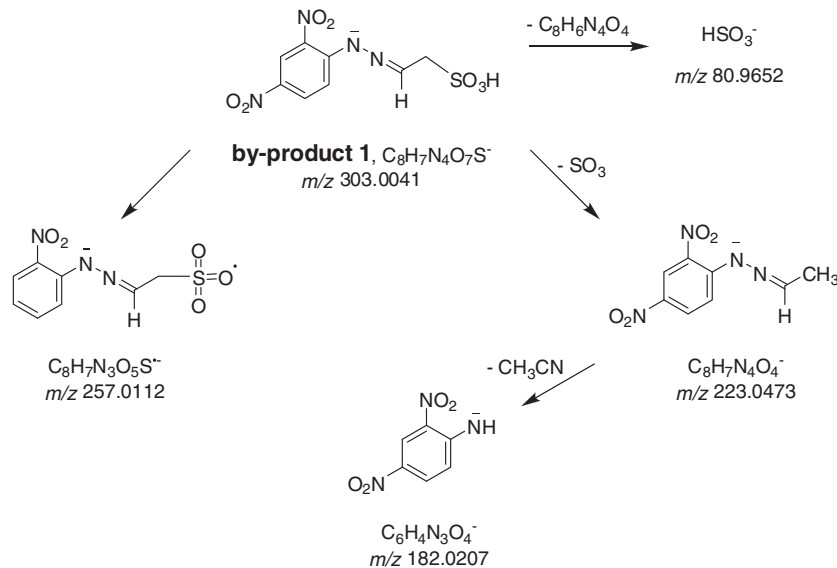
between the two proposed DNPH structures, namely 3,4,5-trioxopentanoic acid and 2,3,4-trioxopentanoic acid.

By-products 6 and 7 showed similar fragmentation patterns. They exhibited [M-H]<sup>-</sup> ions at  $m/z$  297.0101 and 311.0286, associated with elemental compositions of C<sub>9</sub>H<sub>5</sub>N<sub>4</sub>O<sub>8</sub><sup>-</sup> and C<sub>10</sub>H<sub>7</sub>N<sub>4</sub>O<sub>8</sub><sup>-</sup> (error -4.0 and 5.3 ppm), respectively. Both product ion spectra showed two consecutive carbon dioxide eliminations, compatible with a double carboxylation on the DNPH derivative, leading to the formaldehyde derivative at  $m/z$  209.0306 (error -4.9 ppm) and the acetaldehyde derivative at  $m/z$  223.0476 (error 1.4 ppm) for by-products 6 and 7, respectively (Figs. 1(b) and 1(c)). These ions then undergo further fragmentation leading to the ion at  $m/z$  182 (Figs. 4 and 5). For by-product 6 the accurate mass measurement result supported the assignment of a malonic acid derivative with a carbonyl group at the 2-position. For by-product 7, on the other hand, on the basis of the product ion spectrum alone it was not possible to distinguish between two possible dicarboxylic acid structures derivatized at the oxo position, namely 2-formylmalonic acid and 2-oxosuccinic acid. The second possible structure can be also correlated with by-product 4 through an oxidative decarboxylation.

By-product 8 showed a [M-H]<sup>-</sup> ion at  $m/z$  325.0442 consistent with the elemental composition C<sub>11</sub>H<sub>9</sub>N<sub>4</sub>O<sub>8</sub><sup>-</sup> (error 5.0 ppm). The product ion spectrum easily allowed us to assign this by-product as a carboxylated derivative but, once again, it was not possible to unequivocally assign a single structure (Supplementary Fig. S8, Supporting Information). In fact, two product



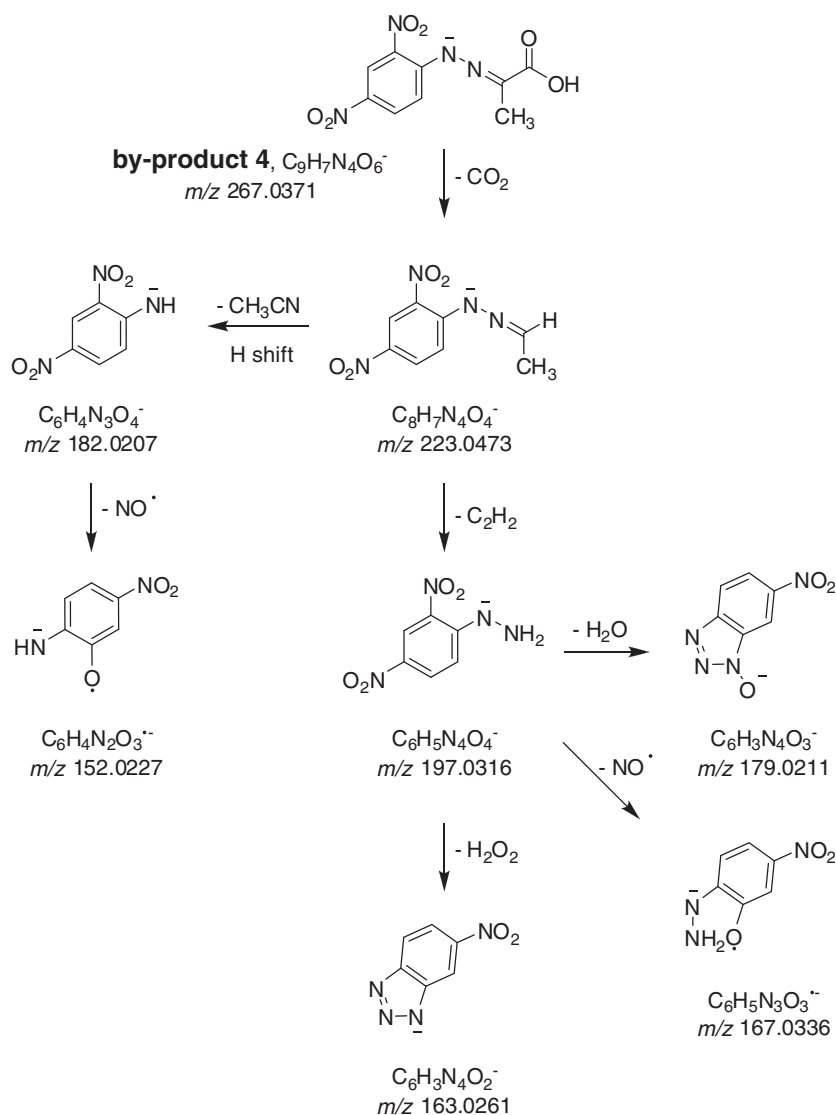
**Figure 1.** Calibrated product ion spectra of (a) by-product 1 (20 eV), (b) by-product 6 (20 eV), (c) by-product 7 (15 eV), and (d) by-product 9 (15 eV). Ions at  $m/z$  182.0207 (by-products 1, 6 and 7) and 252.0374 (by-product 9) were used as lock mass.



**Figure 2.** Proposed fragmentation pathway of by-product 1 from LC/QqTOF-MS/MS data at 20 eV. Accurate mass measurements of product ions are reported in Table 1.

ions are present, at  $m/z$  281.0536 and 253.0184, consistent with a  $\text{CO}_2$  loss (error 3.0 ppm) and  $\text{C}_2\text{H}_4$  elimination (error  $-12.2$  ppm) from  $[\text{M}-\text{H}]^-$ , respectively. Interestingly, accurate

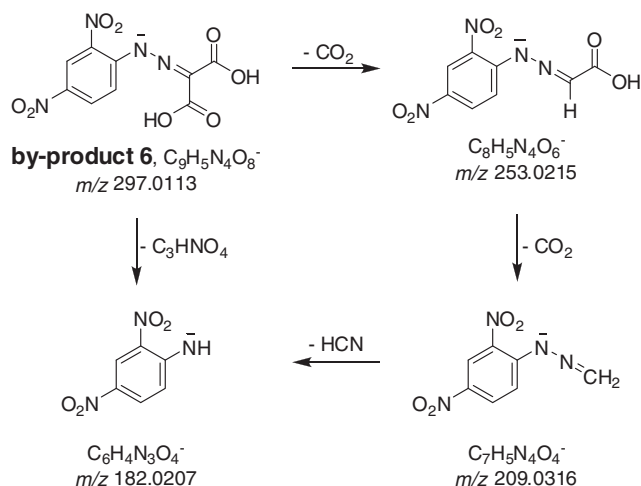
mass measurement of the latter ion made it possible to remove ambiguities between  $\text{CO}$  and  $\text{C}_2\text{H}_4$  elimination from  $[\text{M}-\text{H}]^-$ , both of which have the same nominal mass of 28 Da. A



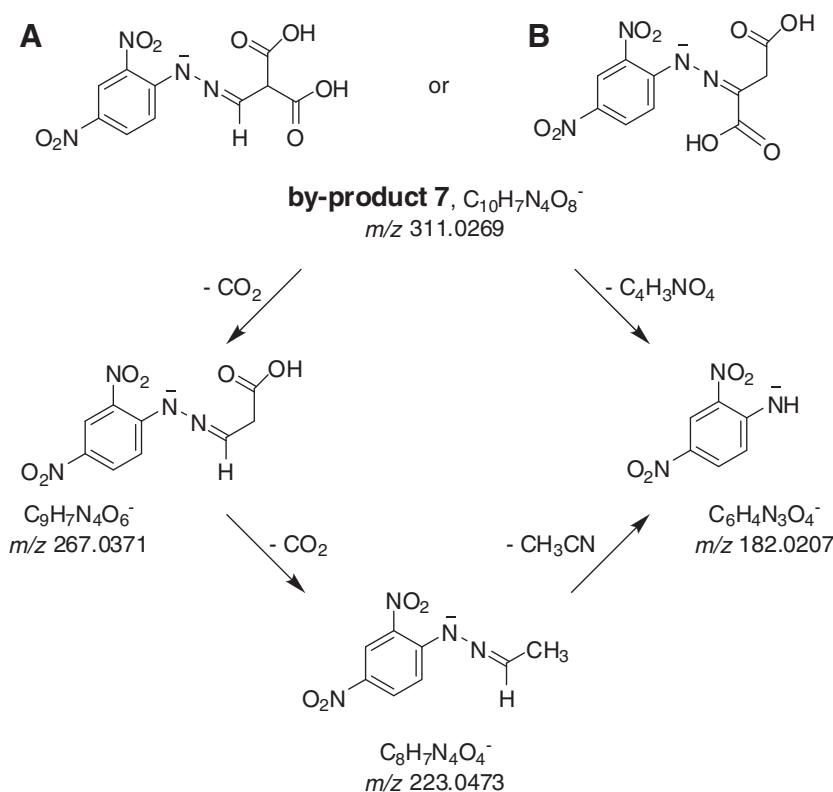
**Figure 3.** Proposed fragmentation pathway of by-product 4 from LC/QqTOF-MS/MS data at 20 eV. Accurate mass measurements of product ions are reported in Table 1.

further fragmentation pathway that is common to that of the 2-oxoacetic acid-DNPH derivative (by-product 3) is depicted in Supplementary Fig. S9 (see Supporting Information).

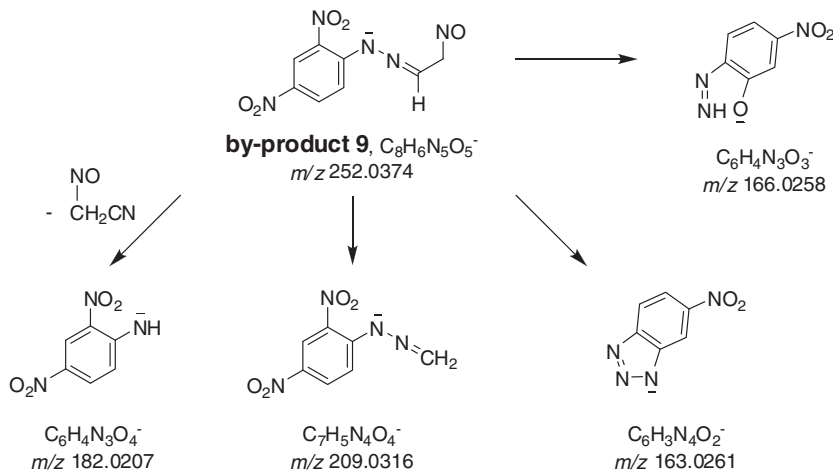
By-products 9 and 10 were shown to be nitrogen-containing compounds. They exhibited  $[M-H]^-$  ions at  $m/z$  252.0366 and 260.0425, associated with elemental compositions of  $C_8H_6N_5O_5^-$  and  $C_{10}H_6N_5O_4^-$  (error  $-3.3$  and  $-0.1$  ppm), respectively. Their structures were rationalized as the DNPH derivatives of 2-nitrosoacetaldehyde and 4-oxobut-2-enitrile, respectively. Their identification confirmed the assumption that nitrogen-containing by-products must be present during the ozonation of Uniblu-OH. In fact, previous experiments employing total nitrogen measurements showed that almost no nitrogen mineralization occurs during the entire reaction time.<sup>[28]</sup> The product ion spectrum of deprotonated by-product 9 (Fig. 1(d)) revealed the presence, in addition to the ion at  $m/z$  182 (base peak), of ions at  $m/z$  209 and 163 typical of aldehyde-DPNH derivatives as discussed above (Fig. 6). The product ion spectrum of deprotonated by-product 10 (Supplementary



**Figure 4.** Proposed fragmentation pathway of by-product 6 from LC/QqTOF-MS/MS data at 20 eV. Accurate mass measurements of product ions are reported in Table 1.



**Figure 5.** Proposed fragmentation pathway of by-product 7 from LC/QqTOF-MS/MS data at 15 eV. Accurate mass measurements of product ions are reported in Table 1.



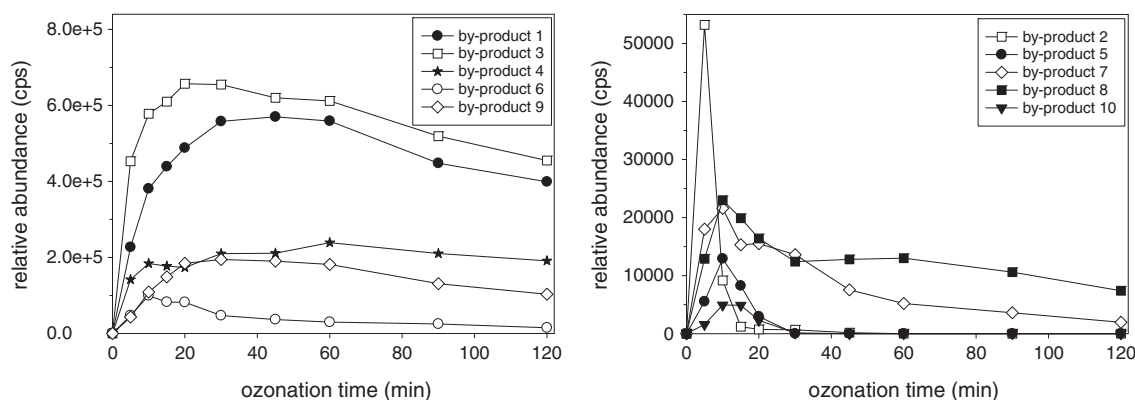
**Figure 6.** Proposed fragmentation pathway of by-product 9 from LC/QqTOF-MS/MS data at 15 eV. Accurate mass measurements of product ions are reported in Table 1.

Fig. S10, Supporting Information) showed a diagnostic ion at  $m/z$  223.0471 (base peak) with elemental composition of  $C_8H_7N_4O_4^-$  (error  $-0.9$  ppm) assigned to acetaldehyde-DNPH that further decomposes to the ion at  $m/z$  182 (Supplementary Fig. S11, Supporting Information).

#### Formation mechanism of identified low molecular weight carbonyl by-products

The identified low molecular weight carbonyl by-products were monitored over a long ozonation time in order to gain

insights about their formation mechanism, and the measured profiles are depicted in Fig. 7. The identified by-products are consistent with further oxidation of the anthraquinone moiety and/or of the benzenesulfoxide group of by-products previously detected in the early stage of Uniblu-OH ozonation.<sup>[28]</sup> It follows that through hydroxylation and subsequent decarboxylation reactions, very polar low molecular weight carbonyl compounds, such as keto-acids and aliphatic aldehydes, are formed. These include newly identified by-products (Table 1) as well as a number of aldehydes of known chemical structure. Specifically, by-products 6, 7 and 8



**Figure 7.** Formation/degradation profiles of identified carbonyl by-products (extracted ion peak area from HPLC-ESI-QqTOFMS) during ozonation of Uniblu-OH.

are likely to be correlated since their structures differ by one methylene group. The most probable mechanism begins with the decarboxylation of by-products 5 and 8 followed by oxidation of the terminal carbon of the formed intermediate, leading ultimately to by-product 7. Such an oxidation is likely to proceed through hydrogen homolytic abstraction by a hydroxyl radical forming a peroxy radical, and then a hydroperoxide. This mechanism can further proceed giving rise to by-product 6 as shown in the degradation pathway (Fig. 8). In addition, the formation of this compound also occurs through degradation of by-product 5 by decarboxylation and oxidation of both the aldehyde and the methyl group (structure A) or homolytic cleavage of the terminal acetyl group and further oxidation (structure B). In addition, cleavage between the keto groups in positions 2 and 3 followed by hydrolysis produces by-product 4 (Fig. 8). It

follows that three of the by-products all lead to a single compound, namely by-product 6. This is also consistent with the formation/decomposition profiles of the identified by-products (Fig. 7), showing that by-product 6 is formed at much higher abundance than by-products 5, 7 and 8. In addition, a further decarboxylation of by-product 6 may lead to by-product 3. Again, this is consistent with the formation/decomposition profiles, showing the latter compound to be persistent at longer reaction time with high abundance.

The same mechanism of decarboxylation and further oxidation discussed above can be applied to by-product 2 in order to explain the formation of by-product 1. This is, once again, consistent with the formation/decomposition profiles showing by-product 1 to be persistent and to be formed at much higher abundance than the other compounds. The finding that sulfur-containing by-products are still present at

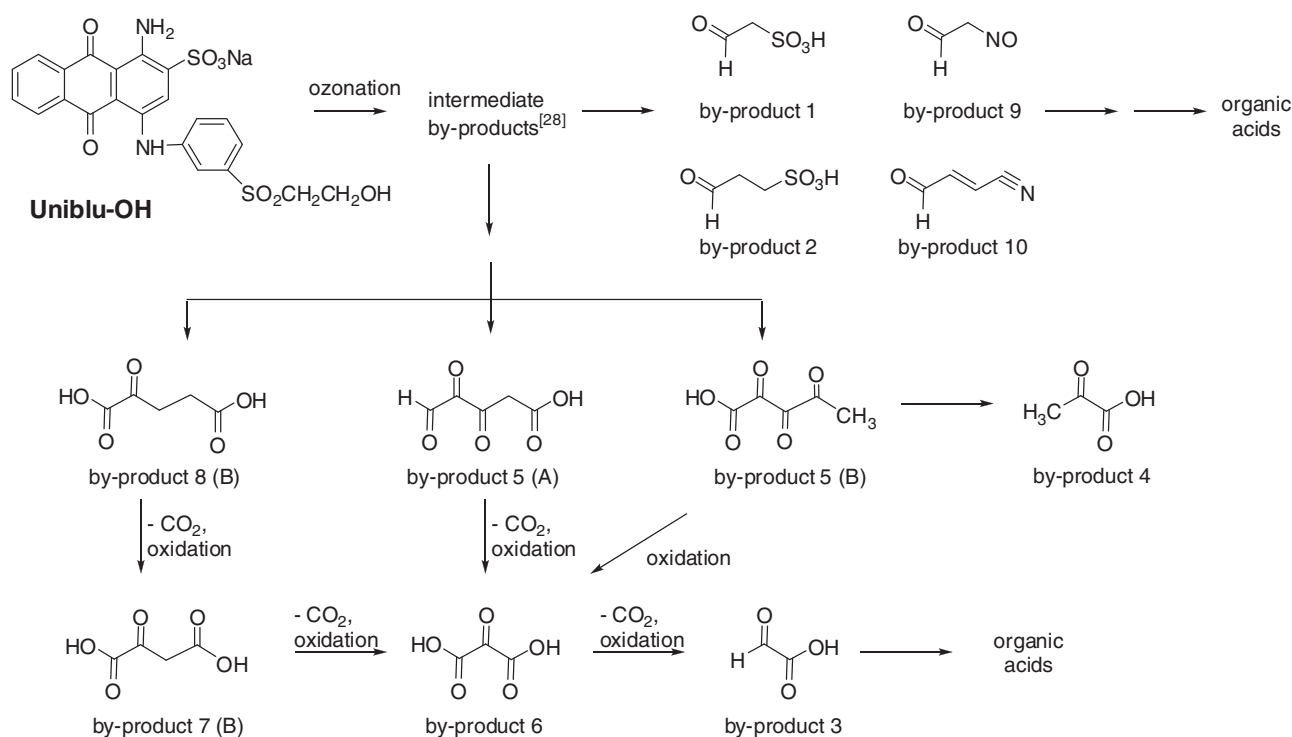


**Figure 8.** Proposed pathway for Uniblu-OH degradation by ozone leading to carbonyl by-products.

longer ozonation time confirms that the sulphur present in Uniblu-OH does not undergo complete mineralization. The concentration of inorganic sulfate alone, in fact, fails to account for the entire organic sulfur balance initially present in the Uniblu-OH.

## CONCLUSIONS

QqTOF-ESI-MS both in single and tandem MS mode, coupled to HPLC, was employed for the characterization of the several polar by-products generated at longer reaction time during the degradation of Uniblu-OH by ozonation. Specifically, the obtained results demonstrated the effectiveness of accurate mass measurements for the identification of by-product structures as well as for obtaining detailed information about their fragmentation patterns. Most of the by-products were characterized by single or double CO<sub>2</sub> loss, consistent with assignment to aldehyde or keto-carboxylic acid structures. The employed experimental approach allowed the identification of both nitrogen- and sulfur-containing carbonyl by-products during Uniblu-OH ozonation. This result is of environmental relevance for the balance of both organic nitrogen and sulfur during the ozonation of Uniblu-OH. These atoms, in fact, do not undergo complete mineralization during AOPs. Owing to the complexity of the reactions occurring during ozonation, it is difficult to draw exhaustive reaction schemes explaining the formation of all the formed by-products. However, it was possible to assess the presence of correlations between different identified by-products, such as aldehyde acids and keto acids. Most of these compounds in turn decompose, through decarboxylation and further oxidation, to smaller homologues. Finally, formation/decomposition profiles confirm that most by-products were further degraded probably leading to the formation of low molecular weight organic acids whose identification is still in progress in our laboratory.

## SUPPORTING INFORMATION

Additional supporting information may be found in the online version of this article.

## Acknowledgement

This work was partially supported by Apulia Region by funding Rela-Valbior project within the Scientific Research Framework Program 2007–2013.

## REFERENCES

- [1] L. S. Andrade, L. A. M. Ruotolo, R. C. Rocha-Filho, N. Bocchi, S. R. Biaggio, J. Iniesta, V. Garcia-Garcia, V. Montiel. On the performance of Fe and Fe, F doped Ti-Pt/PbO<sub>2</sub> electrodes in the electrooxidation of the Blue Reactive 19 dye in simulated textile wastewater. *Chemosphere* **2007**, *66*, 2035.
- [2] W. J. Epolito, Y. H. Lee, L. A. Bottomley, S. G. Pavlostathis. Characterization of the textile anthraquinone dye Reactive Blue 4. *Dyes Pigm.* **2005**, *67*, 35.
- [3] P. R. Gogate, A. B. Pandit. A review of imperative technologies for wastewater treatment II: hybrid methods. *Adv. Environ. Res.* **2004**, *8*, 553.
- [4] M. Pera-Titus, V. Garcia-Molina, M. A. Baños, J. Giménez, S. Espulgas. Degradation of chlorophenols by means of advanced oxidation processes: a general review. *Appl. Catal. B* **2004**, *47*, 219.
- [5] S. Devipriyas, S. Yesodharan. Photocatalytic degradation of pesticide contaminants in water. *Sol. Energy Mater. Sol. Cells* **2005**, *86*, 309.
- [6] J. J. Pignatello, E. Oliveros, A. MacKay. Advanced oxidation processes for organic contaminant destruction based on the Fenton reaction and related chemistry. *Crit. Rev. Environ. Sci. Technol.* **2006**, *36*, 1.
- [7] C. Cominellis, A. Kapalka, S. Malato, S. A. Parsons, I. Poullos, D. Mantzavinos. Perspective. Advanced oxidation processes for water treatment: advances and trends for R&D. *J. Chem. Technol. Biotechnol.* **2008**, *83*, 769.
- [8] M. A. Shannon, P. W. Bohn, M. Elimelech, J. G. Georgiadis, B. J. Mariñas, A. M. Mayes. Science and technology for water purification in the coming decades. *Nature* **2008**, *452*, 301.
- [9] O. J. Hao, H. Kim, P. C. Chiang. Decolorization of wastewater. *Crit. Rev. Environ. Sci. Technol.* **2000**, *30*, 449.
- [10] S. Mondal. Methods of dye removal from dye house effluent – an overview. *Environ. Eng. Sci.* **2008**, *25*, 383.
- [11] J. N. Wu, T. W. Wang. Ozonation of aqueous azo dye in a semi-batch reactor. *Water Res.* **2001**, *35*, 1093.
- [12] M. Koch, A. Yediler, D. Lienert, G. Insel, A. Kettrup. Ozonation of hydrolyzed azo dye Reactive Yellow 84 (CI). *Chemosphere* **2002**, *46*, 109.
- [13] A. Lopez, H. Benbelkacem, J. S. Pic, H. Debellefontaine. Oxidation pathways for ozonation of azo dyes in a semi-batch reactors: a kinetic parameters approach. *Environ. Technol.* **2004**, *25*, 311.
- [14] A. Lopez, G. Ricco, G. Mascolo, G. Tiravanti, A. C. Di Pinto, R. Passino. Biodegradability enhancement of refractory pollutants by ozonation: a laboratory investigation on an azo-dyes intermediate. *Water Sci. Technol.* **1998**, *38*, 239.
- [15] F. F. Zhang, A. Yediler, X. M. Liang. Decomposition pathways and reaction intermediate formation of the purified, hydrolyzed azo reactive dye C.I. Reactive Red 120 during ozonation. *Chemosphere* **2007**, *67*, 712.
- [16] A. Reife, H. S. Freeman. *Environmental Chemistry of Dyes and Pigments*, John Wiley, New York, **1996**.
- [17] F. J. Beltran, *Ozone Reaction Kinetics for Water and Wastewater Systems*, Levis Publishers, Florida, **2004** (imprint of CRC Press LLC).
- [18] O. S. G. P. Soares, J. J. M. Órfão, D. Portela, A. Vieira, M. F. R. Pereira. Ozonation of textile effluents and dye solutions under continuous operation: influence of operating parameters, *J. Hazard. Mater.* **2006**, *137*, 1664.
- [19] D. Deng, J. Guo, G. Zeng, G. Sun. Decolorization of anthraquinone, triphenylmethane and azo dyes by a new isolated *Bacillus cereus* strain DC11. *Int. Biodeter. Biodegr.* **2008**, *62*, 263.
- [20] J. L. Liu, H. J. Luo, C. H. Wei. Degradation of anthraquinone dyes by ozone. *Trans. Nonferr. Metal Soc.* **2007**, *17*, 880.
- [21] Z. Q. He, L. L. Lin, S. Song, M. Xia, L. J. Xu, H. P. Ying, J. M. Chen. Mineralization of C.I. Reactive Blue 19 by ozonation combined with sonolysis: performance optimization and degradation mechanism. *Sep. Purif. Technol.* **2008**, *62*, 376.
- [22] R. Lall, R. Mutharasan, Y. T. Shah, P. Dhurjati. Decolorization of the dye, Reactive Blue 19, using ozonation, ultrasound, and ultrasound-enhanced ozonation. *Water Environ. Res.* **2003**, *75*, 171.

- [23] Y. C. Hsu, Y. F. Chen, J. H. Chen. Decolorization of dye RB-19 solution in a continuous ozone process. *J. Environ. Sci. Health. A* **2004**, *39*, 127.
- [24] J. M. Fanchiang, D. H. Tseng. Decolorization and transformation of anthraquinone dye Reactive Blue 19 by ozonation. *Environ. Technol.* **2009**, *30*, 161.
- [25] J. M. Fanchiang, D. H. Tseng. Degradation of anthraquinone dye C.I. Reactive Blue 19 in aqueous solution by ozonation. *Chemosphere* **2009**, *77*, 214.
- [26] M. Constapel, M. Schellentrager, J. M. Marzinkowski, S. Gáb. Degradation of reactive dyes in wastewater from the textile industry by ozone: Analysis of the products by accurate masses. *Water Res.* **2009**, *43*, 733.
- [27] A. Detomaso, G. Mascolo, A. Lopez. Characterization of carbofuran photodegradation by-products by liquid chromatography/hybrid quadrupole time-of-flight mass spectrometry. *Rapid Commun. Mass Spectrom.* **2005**, *19*, 2193.
- [28] G. Mascolo, A. Lopez, A. Bozzi, G. Tiravanti. By-products formation during the ozonation of the Reactive Dye Uniblu-A. *Ozone Sci. Eng.* **2002**, *24*, 439.
- [29] M. S. van Leeuwen, L. Hendriksen, U. Karst. Determination of aldehydes and ketones using derivatization with 2,4-dinitrophenylhydrazine and liquid chromatography-atmospheric pressure photoionization-mass spectrometry. *J. Chromatogr. A* **2004**, *1058*, 107.
- [30] L. M. Gonçalves, P. J. Magalhães, I. M. Valente, J. G. Pacheco, P. Dostálek, D. Sykora, J. A. Rodrigues, A. A. Barros. Analysis of aldehydes in beer by gas-diffusion microextraction: Characterization by high-performance liquid chromatography-diode-array detection-atmospheric pressure chemical ionization-mass spectrometry. *J. Chromatogr. A* **2010**, *1217*, 3717.
- [31] S. D. Richardson, T. V. Caughran, T. Poiger, Y. B. Guo, F. G. Crumley. Application of DNPH derivatization with LC/MS to the Identification of polar carbonyl disinfection by-products in drinking water. *Ozone Sci. Eng.* **2000**, *22*, 653.
- [32] C. E. Baños, M. Silva. Liquid chromatography-tandem mass spectrometry for the determination of low-molecular mass aldehydes in human urine. *J. Chromatogr. B* **2010**, *878* (7–8), 653.
- [33] R. Andreoli, P. Manini, M. Corradi, A. Mutti, W. M. A. Niessen. Determination of *n*-hexane metabolites by liquid chromatography/mass spectrometry 1. 2,5-Hexanedione and other phase I metabolites in untreated and hydrolyzed urine samples by atmospheric pressure chemical ionization. *Rapid Commun. Mass Spectrom.* **2003**, *17*, 637.
- [34] M. Eggink, M. Wijtmans, R. Ekkebus, H. Lingeman, I. J. P. de Esch, J. Kool, W. M. A. Niessen, H. Irth. Development of a selective ESI-MS derivatization reagent: synthesis and optimization for the analysis of aldehydes in biological mixtures. *Anal. Chem.* **2008**, *80*, 9042.
- [35] P. Manini, R. Andreoli, S. Sforza, C. Dall'Asta, G. Galaverna, A. Mutti, W. M. A. Niessen. Evaluation of Alternate Isotope-Coded Derivatization Assay (AIDA) in the LC-MS/MS analysis of aldehydes in exhaled breath condensate. *J. Chromatogr. B* **2010**, *878*, 2616.
- [36] Methods for the Determination of Organic Compounds in Drinking Water, Method 554. Determination of Carbonyl Compounds in Drinking Water by DNPH Derivatization (HPLC), U.S. Environmental Protection Agency, **1992**.
- [37] E. Grosjean, P. G. Green, D. Grosjean. Liquid Chromatography analysis of carbonyl (2,4-dinitrophenyl) hydrazones with detection by diode-array ultraviolet spectroscopy and by atmospheric pressure negative chemical ionization mass spectrometry. *Anal. Chem.* **1999**, *71*, 1851.
- [38] S. Kolliker, M. Oheme. Structure elucidation of 2,4-dinitrophenylhydrazone derivatives of carbonyl compounds in ambient air by HPLC/MS and multiple MS/MS using atmospheric chemical ionization in the negative ion mode. *Anal. Chem.* **1998**, *70*, 1979.
- [39] C. Zwiener, T. Glauner, F. H. Frimmel. Method optimization for the determination of carbonyl compounds in disinfected water by DNPH derivatization and LC-ESI-MS-MS. *Bioanal. Chem.* **2002**, *372*, 615.